Nanoscale Res Lett (2007) 2:550–553
DOI 10.1007/s11671-007-9097-x

NANO EXPRESS

Multiple Wavelength InGaAs Quantum Dot Lasers Using Ion Implantation Induced Intermixing

S. Mokkapati · Sichao Du · M. Buda · L. Fu · H. H. Tan · C. Jagadish

Received: 27 August 2007 / Accepted: 6 September 2007 / Published online: 25 September 2007

Abstract We demonstrate multiple wavelength InGaAs quantum dot lasers using ion implantation induced intermixing. Proton implantation, followed by annealing is used to create differential interdiffusion in the active region of the devices. The characteristics (lasing-spectra, threshold currents and slope efficiencies) of the multi-wavelength devices are compared to those of as-grown devices and the differences are explained in terms of altered energy level spacing in the annealed quantum dots.

Keywords Quantum dot lasers · Ion implantation

Integration of several quantum dot (QD) devices on a single chip offers the advantages of compact size, high speed and low optical losses, added to the advantages discrete QD devices offer due to three-dimensional carrier confinement in the active region. Ion implantation induced intermixing is a technique that is compatible with planar processing and can be used for band gap tuning, essential for device integration. Ion implantation induced intermixing has been widely used for band gap tuning of quantum wells [1, 2] (QW) and QDs [3–8]. QW based integrated photonic devices have also been demonstrated using implantation induced intermixing [9, 10]. Though there are many reports on band gap tuning of QDs, there are no reports to date on multi-color QD lasers using ion implantation induced intermixing. In this letter, we report on multi-wavelength QD lasers fabricated using implantation induced intermixing. We first demonstrate differential band gap shift and effect on carrier confinement and energy level spacing in QDs due to ion implantation induced intermixing, using photoluminescence (PL). Then we report on multi-color QD lasers and discuss the effect of intermixing induced changes in confinement and energy level separation in the active region on the performance of the devices.

The thin p-clad laser structures studied in this work were grown by metal-organic chemical vapor deposition (MOCVD) system. Trimethylindium, trimethylgallium and AsH_3 with H_2 as the carrier gas were used as the precursor sources; Silane and CCl_4 were used as n- and p-type dopant sources, respectively. The active region of the lasers consisted of five layers of $In_{0.5}Ga_{0.5}As$ QDs incorporated into GaAs barrier layers. 100 keV protons at a dose of 5×10^{13} cm^{-2} were implanted into the active region, wherever mentioned. Following implantation, the device structures were annealed at 600 °C for 30 min in the presence of AsH_3. Annealing conditions were chosen to maximize the room temperature (RT) PL recovery from the QDs in the active region. PL spectra from the active region of the devices were obtained prior to device fabrication by exciting the samples using a 635 nm laser and collecting the luminescence using a cooled InGaAs detector. Four micrometers wide ridge wave-guide lasers were fabricated from the annealed and as-grown laser structures using the standard device processing steps [11]. The as-cleaved devices were tested at RT in pulsed mode (duty cycle 5%).

First, we present results demonstrating differential band gap shift and the effect of annealing on the carrier confinement and separation between consecutive energy levels

S. Mokkapati (✉) · S. Du · L. Fu · H. H. Tan · C. Jagadish
Department of Electronic Materials Engineering, Research School of Physical Sciences and Engineering, The Australian National University, Canberra, ACT 0200, Australia
e-mail: smokkapati@ieee.org

M. Buda
National Institute of Materials Physics, Str. Atomistilor 105bis, P.O. Box MG-7, Magurele 077125, Romania

in the QDs in the active region of the laser structure. Due to larger effective mass of holes compared to that of electrons, the hole energy levels are closely spaced than the electron energy levels and holes are less confined than the electrons in the as-grown sample. Interdiffusion has the same effect on hole energy levels as that on electron energy levels, but we only discuss the effect of interdiffusion on carriers with higher confinement (electrons), as the device performance is affected mainly by changes in electron confinement rather than the hole confinement. Figure 1 shows the 10 K PL spectra from the active region of the device structures annealed with and without implantation. For the un-implanted region, the QD ground state (GS) luminescence peaks at 1015 nm (P1). Due to enhanced interdiffusion caused by proton implantation, the QD GS luminescence peak (P1′) from the implanted region is blue shifted with respect to peak P1 from the un-implanted region. Under the implantation and annealing conditions used in this study, the differential shift is ~19 meV. Peaks P2 and P2′ represent QD excited state (ES) transitions in un-implanted and implanted samples, respectively. The wetting layer transitions appear at shorter wavelengths and are denoted as P3 and P3′ for the un-implanted and implanted samples, respectively.

The carrier confinement in the active region of the devices is determined by the separation between the GaAs (barrier) band edge and the QD energy levels (E_{conf} in Fig. 1). Assuming a conduction band offset of $0.6E_g$, the confinement energy for the electrons occupying the lowest energy level in the conduction band of QDs in the as-grown device structure is ~230 meV (not shown), whereas the confinement energy for the carriers occupying the GS of QDs in the un-implanted and implanted, annealed devices is ~180 meV and 168 meV, respectively. Thermal population of QD ES depends on the energy separation between the GS and ES (ΔE in Fig. 1). The separation between consecutive energy levels in the conduction band calculated from the observed peaks in the PL spectra from both implanted (P1′ and P2′) and un-implanted (P1 and P2) samples is ~35 meV, which is very close to the thermal energy of carriers at RT. These results indicate that the carriers in the annealed quantum dots have smaller confinement energy and greater probability of occupying ES.

We now present results demonstrating multi-color lasing from the QD lasers fabricated using ion implantation induced intermixing and compare their characteristics with as-grown devices. Figure 2 shows the lasing spectra of 2 mm long lasers fabricated from un-implanted and implanted device structures. The lasing spectrum of an as-grown device is also shown as a reference. The blue shift between the spectra of as-grown device and annealed only device is a result of interdiffusion due to background (grown-in) defect levels, whereas the shift between the annealed only device and device annealed after implantation is due to implantation induced differential band gap shift. The spectra of implanted and un-implanted devices are shifted with respect to each other by ~40 meV. This shift is greater than the shift in the QD PL peak positions indicated by the dashed vertical lines in Fig. 1. It is also interesting to note from Fig. 2 that the annealed devices have broader lasing spectra compared to that of the as-grown devices. Broad lasing spectra could be a consequence of high injection current densities required for lasing in the annealed devices [12].

Simultaneous lasing from different energy levels in QD or QW lasers has been observed by several groups [13–16], especially for short cavity lengths and was explained in terms of high cavity losses, which lead to increase in

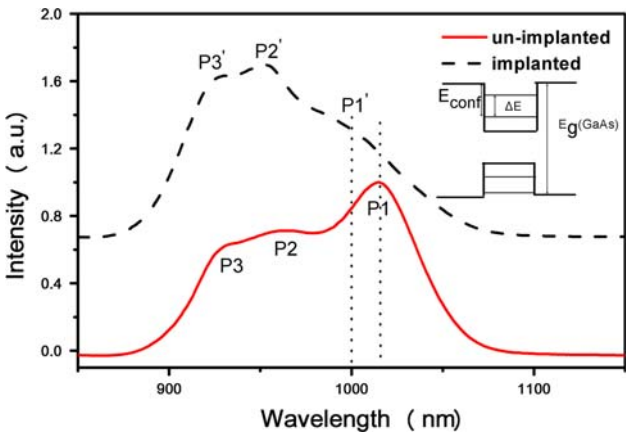

Fig. 1 Photoluminescence spectra at 10 K from the active region of the device structures annealed with or without implantation. Inset schematically defines the energy terms (ΔE and E_{conf}) used in the text

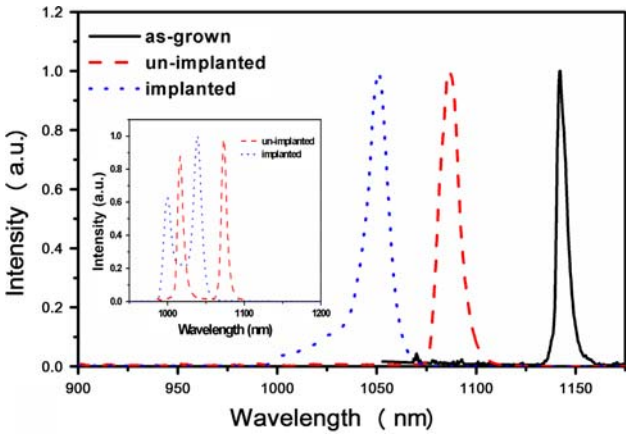

Fig. 2 Lasing spectra of 2 mm long lasers fabricated from as-grown; un-implanted, annealed and implanted, annealed device structures. Inset shows lasing spectra of 1 mm long laser fabricated from implanted and un-implanted, annealed device structures

threshold and thus to increased band filling [15]. Increasing the operation temperature would also require higher injection and leads to the same effect [16]. At RT, the as-grown devices studied in this work lase from QD GS for all cavity lengths whereas the annealed devices show simultaneous lasing from different energy levels (for $L \leq 1.5$ mm for un-implanted and $L \leq 2$ mm for implanted devices). Inset in Fig. 2 shows the lasing spectra of 1 mm long devices fabricated from annealed device structures (with or without implantation). As will be discussed later, the annealed devices have higher thresholds (consequence of smaller E_{conf} and ΔE) leading to increased band filling. Also, smaller values of ΔE in the annealed QDs increase the probability of thermal population of higher energy levels. So we attribute simultaneous lasing from different energy levels in the annealed devices to modification of energy level separation in the active region, as a consequence of annealing.

Figure 3 shows the threshold current densities of as-grown, un-implanted, annealed and implanted, annealed devices. The implanted and un-implanted devices have similar threshold current densities, suggesting that at the implantation conditions used, there are no additional residual defects in the implanted devices after annealing. The annealed (both implanted and un-implanted) devices have higher threshold current densities than the as-grown devices for any given cavity length. The annealed devices also have lower slope efficiencies than the as-grown devices (inset of Fig. 3). From 5 °C to 20 °C, the slope efficiency of a 3 mm long un-implanted, annealed device changes by 89%, while that of an as-grown device of same length changes by only 30% by increasing the temperature from 5 °C to 55 °C. The smaller separation between consecutive energy levels (ΔE) in the annealed QDs cause loss

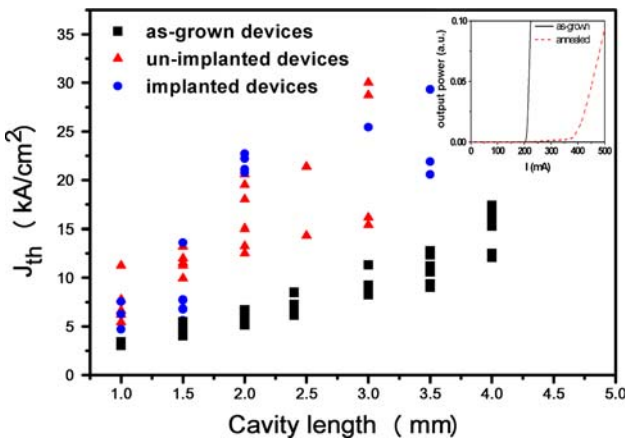

Fig. 3 Threshold current density versus cavity length for as-grown; un-implanted, annealed and implanted annealed lasers. Inset shows the output power (L) versus injected current (I) plots for as-grown and annealed devices (cavity length: 3 mm)

of carriers from lower (lasing) energy states to higher energy states, reducing the net gain available from these states. Increased thermal population of higher energy states in the barrier/WL (smaller values of E_{conf}) increases the fraction of injected carriers that can access non-radiative recombination paths [17]. The loss of carriers from the lasing states to higher energy levels in the QDs/WL/barrier results in increased threshold currents and lower slope efficiencies in the annealed devices. The fraction of carriers lost from the lasing states to states that do not contribute to lasing increases with increasing temperature as [exp $(-E/k_BT)$], where E is the energy separation between the lasing and non-lasing energy states. The rate of loss of carriers is higher in annealed samples because of smaller values of ΔE and E_{conf}, resulting in a rapid decrease in the slope efficiency with temperature, compared to the as-grown sample.

The above results indicate that smaller values of ΔE and E_{conf} in the multiple-wavelength devices result in poor performance compared to the as-grown devices. Improvement in device performance has been reported by engineering the QD energy levels [18] (to increase ΔE) and using AlGaAs barriers [19] (to increase E_{conf}). We believe that using similar approaches with implantation induced intermixing may result in multi-color lasers with improved characteristics.

In summary, we have demonstrated multiple wavelength InGaAs QD lasers using ion implantation induced intermixing. For a cavity length of 2 mm, the shift in the lasing wavelength of un-implanted and implanted devices is 40 meV. Implantation followed by annealing of device structures used for achieving differential band gap shift alters the energy level spacing in the active-region, resulting in broader lasing spectra, higher threshold current densities and lower slope efficiencies with respect to the as-grown devices. Hence band gap tuning using ion implantation induced intermixing requires careful design of devices to minimize carrier loss from the QD active region.

Thanks are due to Marie Bruneau, Michael Aggett for expert technical advice. The Australian Research Council is gratefully acknowledged for the financial support.

References

1. P.G. Piva, P.J. Poole, M. Buchanan, G. Champion, I. Templeton, G.C. Aers, R. Williams, Z.R. Wasilewski, E.S. Koteles, S. Charbonneau, Appl. Phys. Lett. **65**, 621 (1994)
2. S. Charbonneau, P.J. Poole, Y. Feng, G.C. Aers, M. Dion, M. Davies, R.D. Goldberg, I.V. Mitchell, Appl. Phys. Lett. **67**, 2954 (1995)
3. T. Surkova, A. Patanè, L. Eaves, P.C. Main, M. Henini, A. Polimeni, A.P. Knights, C. Jeynes, J. Appl. Phys. **89**, 6044 (2001)
4. B. Salem, V. Aimez, D. Morris, A. Turala, P. Regreny, M. Gendry, Appl. Phys. Lett. **87**, 241115 (2005)

5. S. Fafard, C. Nì. Allen, Appl. Phys. Lett. **75**, 2374 (1999)
6. P. Lever, H.H. Tan, C. Jagadish, P. Reece, M. Gal, Appl. Phys. Lett. **82**, 2053 (2003)
7. S. Barik, H.H. Tan, C. Jagadish, Appl. Phys. Lett. **88**, 223101 (2006)
8. C. Dion, P. Desjardins, M. Chicoine, F. Cshiettekatte, P.J. Poole, S. Raymond, Nanotechnology **18**, 015404 (2007)
9. H.H. Tan, C. Jagadish, Appl. Phys. Lett. **71**, 2680 (1997)
10. S. Charbonneau, P.J. Poole, P.G. Piva, G.C. Aers, E.S. Koteles, M. Fallahi, J.J. He, J.P. McCaffrey, M. Buchanan, M. Dion, R.D. Goldberg, I.V. Mitchell, J. Appl. Phys. **78**, 3697 (1995)
11. M. Buda, J. Hay, H.H. Tan, J. Wong-Leung, C. Jagadish, IEEE J. Quantum Electron. **39**, 625 (2003)
12. M. Sugawara, N. Hatori, H. Ebe, M. Ishida, Y. Arakawa, T. Akiyama, K. Otsubo, Y. Nakata, J. Appl. Phys. **97**, 043523 (2005)
13. L.F. Lester, A. Stintz, H. Li, T.C. Newell, E.A. Pease, B.A. Fuchs, K.J. Malloy, IEEE Photon. Tech. Lett. **11**, 931 (1999)
14. F. Karouta, E. Smalbrugge, W.C. van der Vleuten, S. Gaillard, G.A. Acket, IEEE J. Quantum Electron. **34**, 1474 (1998)
15. M. Mittlestein, Y. Arakawa, A. Larsson, A. Yariv, Appl. Phys. Lett. **49**, 1689 (1986)
16. P.S. Zory, A.R. Reisinger, R.G. Waters, L.J. Mawst, C.A. Zmudzinski, M.A. Emanuel, M.E. Givens, J.J. Coleman, Appl. Phys. Lett. **49**, 16 (1986)
17. D.G. Deppe, D.L. Huffaker, S. Csutak, Z. Zou, G. Park, O.B. Shchekin, IEEE J. Quantum Electron. **35**, 1238 (1999)
18. O.B. Shchekin, G. Park, D.L. Huffaker, D.G. Deppe, Appl. Phys. Lett. **77**, 466 (2000)
19. S.V. Zaitsev, N.Y. Gordeev, V.I. Kopchatov, V.M. Ustinov, A.E. Zhukov, A.Y. Egorov, N.N. Ledentsov, M.V. Maximov, P.S. Kop'ev, A.O. Kosogov, Z.I. Alferov, Jpn. J. Appl. Phys. **36**, 4219 (1997)